ELSEVIER

Polymer 42 (2001) 9763–9769

polymer

www.elsevier.com/locate/polymer

The novel polymer electrolyte nanocomposite composed of poly(ethylene oxide), lithium triflate and mineral clay

Hsien-Wei Chen, Feng-Chih Chang*

Institute of Applied Chemistry, National Chiao-Tung University, Hsin-Chu, Taiwan, 30043

Received 3 April 2001; received in revised form 14 June 2001; accepted 13 July 2001

Abstract

This work has demonstrated that the addition of optimum content of D-2000 modified montmorillonite enhances the ionic conductivity of the poly(ethyl oxide) (PEO) based electrolyte by nearly sixteen times more than the plain system. Specific interactions among silicate layer, ethyl oxide and lithium cation have been investigated using alternating current impedance (A.C. impedance), differential scanning calorimetry (DSC) and Fourier-transform infrared (FT-IR). The DSC characterization confirms that the initial addition of clay is able to enhance the PEO crystallinity due to the interaction between the negative charge from the clay and the lithium cation. Three types of complexes are present; complex I is present in the PEO phase, complex II resides at the interphase, and complex III is located within the clay domain. Complex II plays the key role in stabilizing these two microstructure phases. FT-IR spectra confirm that the existence of clay is able to dissolve the lithium salts, easier than the plain electrolyte system and thus increases the fraction of free ions. © 2001 Published by Elsevier Science Ltd.

Keywords: Polymeric electrolytes; Ionic conductivity; Clay

1. Introduction

During the past decade, considerable effort has been devoted to the development of solid polymer electrolytes with high ionic conductivity at room temperature [1–8]. The major motivation for this interest is a technological application in rechargeable and high energy density power sources. poly(ethylene oxide) (PEO) based polymeric electrolytes are still among the most extensively studied polymer ionic conductors due to the beneficial structure in supporting fast ion transport [2,9–14]. Unfortunately, a high crystalline phase concentration, limits the conductivity of PEO based electrolytes; this is mainly due to the basic requirement for ionic mobility. Various methods have been applied to reduce the crystallinity of PEO based electrolytes while maintaining their high flexibility and mechanical stability, which extends over a wide temperature range. One of the most successful approaches relies on the preparation of polymer electrolyte nanocomposite [9,15–25]. Clay mineral is an inorganic filler with intercalation property. Intercalating polymer in layered clay host can produce polymer electrolyte nanocomposite, with huge interfacial area. The higher interfacial area not only reduces the crystallinity of PEO chains resulting in higher ionic conductivity, but also sustains the mechanical property of this semi-crystalline PEO based electrolyte. However, the mechanism of such ionic conductivity enhancement is not clearly understood. In the work, via alternating current (A.C.) impedance, differential scanning calorimetry (DSC) and Fourier-transform infrared (FT-IR), the complicated solid-state interaction between PEO, lithium triflate salt ($LiCF_3SO_3$) is clarified. In addition, changes in PEO crystallinity of the composite system will be discussed through the formation of three types of complexes. Furthermore, these three different types of complexes are employed to interpret the interaction between ethyl oxide, clay mineral and lithium cation. The purpose of this work is to emphasize the extraordinary effect occurring when the clay is added to the PEO/clay/Li^+ blend system.

2. Experimental section

2.1. Sample preparation

The PEO with weight average molecular weight of 200,000 was purchased from Aldrich. The lithium triflate ($LiCF_3SO_3$, LiTf) also purchased from Aldrich was dried in

* Corresponding author. Tel.: +886-35-712-121 ext. 56502; fax: 886-35-723-764.

E-mail address: changfc@cc.nctu.edu.tw (F.-C. Chang).

0032-3861/01/$ - see front matter © 2001 Published by Elsevier Science Ltd.
PII: S0032-3861(01)00520-1

a vacuum oven at 80°C for 24 h and then stored in a desiccator, prior to use. Acetonitrile was refluxed at a suitable temperature under nitrogen atmosphere, prior to use. Poly(oxypropylene) diamine (the trade name is D-2000, $M_n = 2000$) was purchased from Huntsman Co. in United States.

2.2. Preparation of mineral clay

0.5 mol of the D-2000 diamine was acidified by hydrochloric acid (HCl). The clay, sodium montmorillonite (1 g), and 50 ml distilled water were placed in a 100 ml beaker, and 2.3 g of acidified D-2000 was added to the solution (Clay/D-2000 = 1/1). The mixture was stirred vigorously for 8 h, filtered and washed with deionized water. The modified clay was dried in a vacuum oven at 60°C for 24 h. Notably, the D-2000 modified montmorillonite is highly hydrophobic.

2.3. X-ray measurements

Wide-angle diffraction (WAXD) experiments were conducted on a Rigaku X-ray Diffractmeter that employed Cu-Kα radiation (18 kw rotating anode, $\lambda = 1.5405$ Å), and were performed at 50 kV and 250 mA with a scanning rate of 2 deg min^{-1}.

2.4. Preparation of solid polymer electrolyte (SPE)

Desired amount of PEO, vacuum dried $LiCF_3SO_3$ salt and clay in dry acetonitrile were mixed to form PEO/clay/$LiCF_3SO_3$ nanocomposites of varying compositions. Following continuous stirring for 24 h at 80°C, these solutions were maintained at 50°C for an additional period of 24 h to facilitate initial de-solvent. Further drying was carried out under vacuum at 70°C for three days. To prevent contact with air and moisture, all nanocomposites were stored in a dry box filled with nitrogen. All samples were equilibrated at ambient temperature for at least 1 month in a dry box before undertaking any further experiment.

2.5. Conductivity measurements

Ionic conductivity measurements with alternating current were conducted on an AUTOLAB, designed by Eco Chemie within the frequency range 10 MHz to 10 Hz. The composite film was sandwiched between stainless steel blocking electrodes (1 cm diameter). The specimen thickness varied from 0.8 to 1.2 mm, and the impedance response was gauged over the range 20–120°C.

2.6. Differential scanning calorimetry (DSC)

Thermal behavior of PEO based electrolyte films were characterized by a DSC from Du-Pont (DSC-9000) equipped with a low-temperature measuring head and a liquid nitrogen-cooled heating element. About 30–60 mg sample in a aluminum pan was stabilized by slow cooling to −110°C and then heated at 10°C min^{-1} to 200°C.

The PEO crystallinity of the electrolyte film was calculated as a ratio of the heat enthalpy of the crystalline PEO phase to the heat enthalpy of the pure crystalline PEO (165.5 J g^{-1}) [9,26,27].

2.7. Infrared spectroscopy

The conventional NaCl disk method was employed to measure the infrared spectra of composite films. All polymer films were prepared within N_2 atmosphere. The acetonitrile solution was cast onto a NaCl disk from which the solvent was removed under vacuum at 70°C, for 48 h. All infrared spectra were obtained at a resolution of 1 cm^{-1} on a Nicolet AVATAR 320 FTIR Spectrometer at 120°C.

3. Results and discussions

3.1. Nanocomposite structures

Depending on the method of preparation, different interlayer spacing may be obtained when a layered clay is associated with a polymer. In such nanocomposites, the repetitive multiplayer structure is well preserved, allowing the interlayer spacing to be determined. X-ray technique is often applied to identify intercalated structures through the Bragg's relation:

$$\lambda = 2d \sin \theta$$

where λ corresponds to the wave length of the X-ray radiation ($\lambda = 1.5405$ Å) used in the diffraction experiment, d corresponds to the spacing between diffractional lattice planes and θ is the measured diffraction angle.

Fig. 1(a) and (b) present the X-ray diffraction patterns for the blank clay and the D-2000 modified montmorillonite (organoclay). Upon intercalation, the basal spacing expanded from 1.24 to 2.07 nm indicating the incorporation of large surfactant molecules (D-2000). Fig. 1(c) presents that the interlayer spacing of PEO/clay = 97/3 system is 2.41 nm, higher than the spacing of the organoclay used (2.07 nm). Fig. 1(d) and (e) show lower interlayer spacing with further increase of clay content in the PEO/clay system. The phenomenon of lower interlayer spacing with higher percentage of clay could be attributed to the less polymer chains, intercalate within the galleries. It is worth to point out that the PEO/clay blends are the nanosized composites, and that these nanocomposites exhibit marked surface area of silicate layers.

3.2. Conductivity

Fig. 2 presents the Arrhenius plots which illustrates the temperature dependence on the ionic conductivity for the $(PEO)_8LiCF_3SO_3$/clay electrolyte nanocomposites,

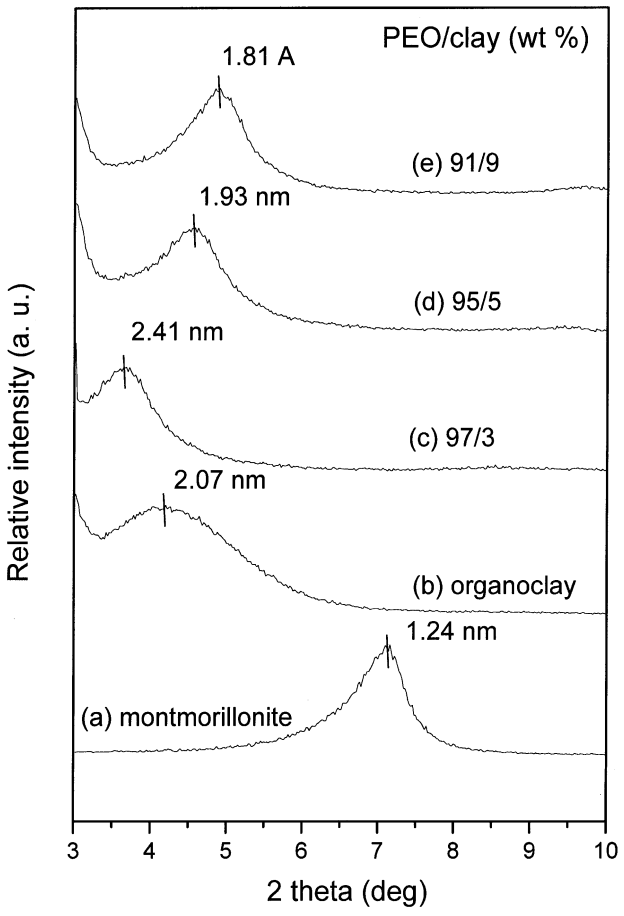

Fig. 1. WAXD patterns of (a) montmorillonite; (b) organoclay; (c) PEO/clay = 97/3; (d) PEO/clay = 95/5; (e) PEO/clay = 91/9.

containing various clay concentrations. The conductivity increases with the increase of the clay content and attains a maximum value when the clay concentration is at 3%. Subsequently, the conductivity decreases drastically with

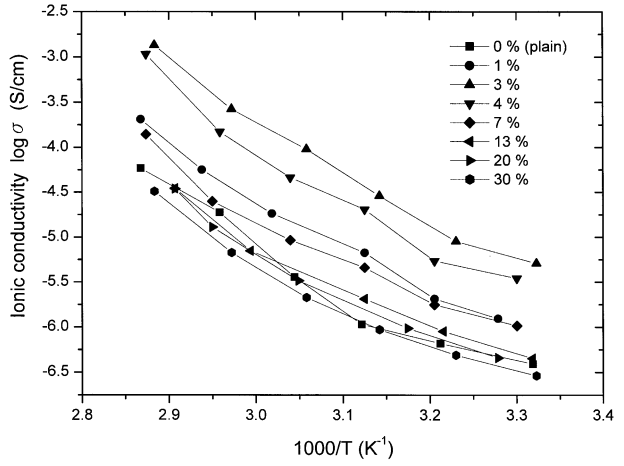

Fig. 2. Arrhenius conductivity plots for PEO/clay/$LiCF_3SO_3$ composite electrolyte containing various clay concentration (wt%): (■) 0%; (●) 1%; (▲) 3%; (▼) 4%; (◆) 7%; (◄) 13%; (►) 20%; (⬢) 30%; (where $EO/Li^+ = 8$).

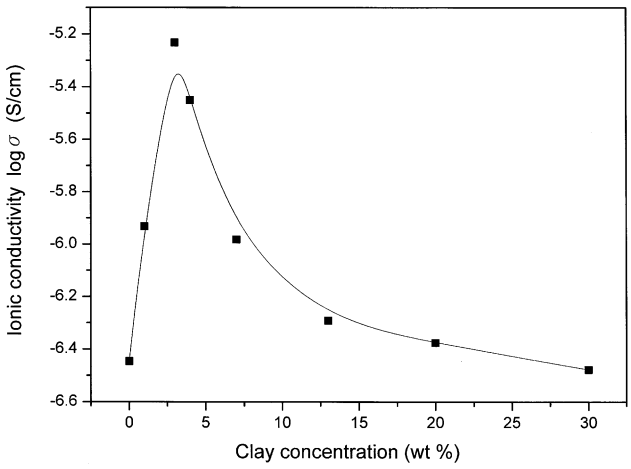

Fig. 3. Ionic conductivity versus clay concentration (wt%) for PEO/clay/$LiCF_3SO_3$ composite electrolytes at 30°C (where $EO/Li^+ = 8$).

further increase in the clay content. Fig. 3 plots the conductivity versus clay content for the $(PEO)_8(LiCF_3SO_3)$/clay composite electrolytes, at 30°C. A rapid increase in the conductivity is observed by adding small quantity of the clay and the maximum ionic conductivity is at 3% clay concentration. When the clay is increased to 13% or higher, the conductivity decreases to near its original value. Plots of log σ versus ethylene oxide/Li^+ ratio (EO/Li^+ ratio) for the plain ($PEO/LiCF_3SO_3$) and the composite (PEO/clay/$LiCF_3SO_3$) electrolyte systems, are shown in Fig. 4. The conductivity of the plain electrolyte system increases initially with decreasing EO/Li^+ ratio and reaches maximum value at the EO/Li^+ ratio of 8 but decreases as the EO/Li^+ ratio is further decreased. This conductivity behavior is consistent with the generally observed behavior of polymer salt electrolytes. This phenomenon is attributed to an initial increase in the number of charge carriers, followed by the formation of less mobile ionic aggregates, as the salt concentration is further increased. However, the

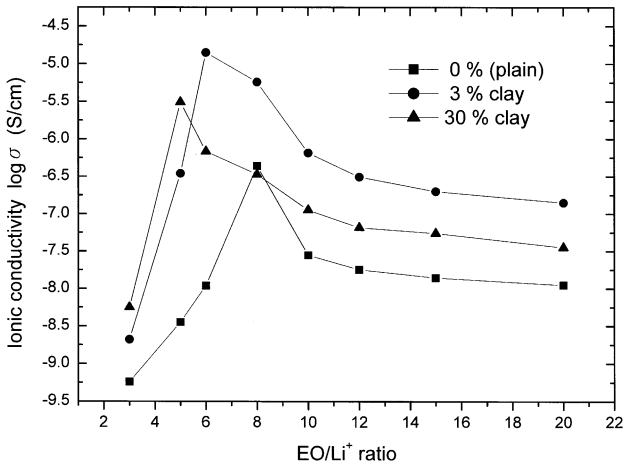

Fig. 4. Ionic conductivity versus EO/Li^+ ratio for PEO/clay/$LiCF_3SO_3$ composite electrolytes containing various clay concentration (wt%) at 30°C: (■) 0%; (●) 3%; (▲) 30%.

critical EO/Li^+ ratio, to achieve the maximum conductivity, shifts lower with the clay presence, as shown in Fig. 4. The presence of negative charges in the silicate layers is able to effectively disperse the salt throughout the blend and impedes the ionic aggregation process. These negative charges existing in the silicate layers, play the same role as the polar group in PEO. In other words, the PEO/clay/$LiCF_3SO_3$ composite electrolyte is able to dissolve more lithium salt and causes the optimum EO/Li^+ ratio decreasing (higher lithium salt concentration).

It is worthy to note that the optimum ionic conductivity with 30% clay (3×10^{-6} S cm^{-1}) is lower than the system with 3% clay (1.4×10^{-5} S cm^{-1}). This phenomenon can be attributed to the fact that excess clay content may clutch the lithium cation tightly, and thus restricts the mobility of the cation and decreases the ionic conductivity. The optimum ionic conductivity is obtained from the balanced attractive forces among silicate layers, ethyl oxide groups and lithium cations, and thus the optimum clay content varies with systems.

3.3. DSC studies

Fig. 5 presents the DSC curves for the pure, undoped PEO

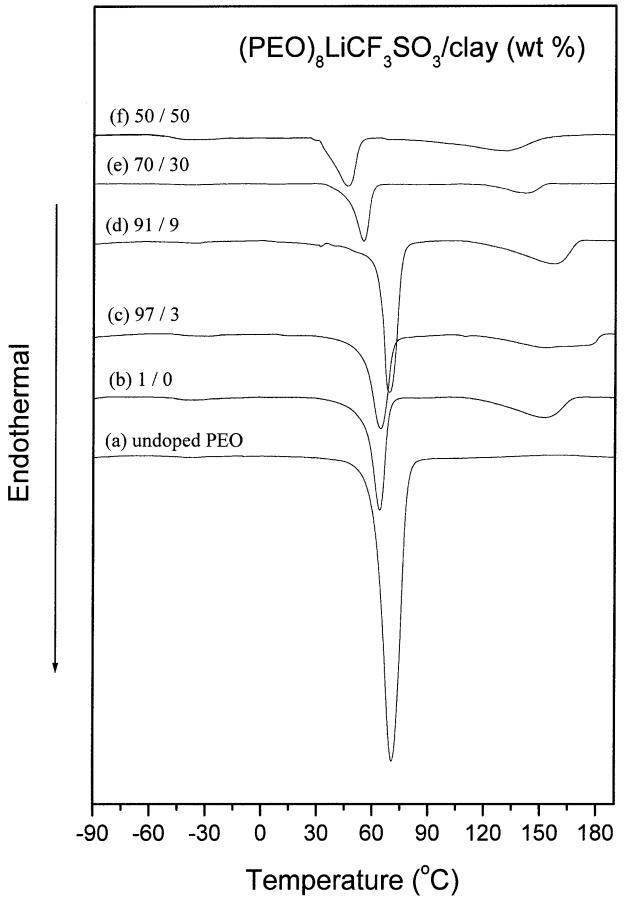

Fig. 5. DSC trances obtained for PEO/clay/$LiCF_3SO_3$ composite electrolytes containing various clay concentration (wt%): (a) undoped PEO; (b) 0%; (c) 3%; (d) 9%; (e) 30%; (f) 50% (where EO/Li^+ = 8).

Table 1
DSC data for PEO/clay/$LiCF_3SO_3$ composite polymeric electrolytes [where, EO/Li^+ = 8]

wt%[a]	T_g (°C)	T_m (°C)	ΔH_m (J g^{-1})	X_c (%)	T_{mc} (°C)
0[b]		70.50	165.5		
0	− 46	59.84	59.9	36.2	152.0
3	− 50	71.58	68.9	41.6	149.7
9	− 43	77.74	77.8	47.0	156.9
30	− 46	54.93	40.1	24.2	142.6
50	− 48	45.99	29.1	17.6	132.4

[a] Concentration of clay in wt%.
[b] Undoped PEO sample.

(Fig. 5(a)), the $(PEO)_8(LiCF_3SO_3)$ electrolyte (Fig. 5(b)), and the $(PEO)_8(LiCF_3SO_3)$/clay system containing 3, 9, 30 and 50 wt% of clay. DSC results are summarized in Table 1. Similar curves have been obtained for other electrolytes [9,26,27]. Two endothermic first order transitions can be observed, except the undoped PEO. The undoped PEO has only one first order transition at ~70°C, corresponding to the melting of the crystalline PEO phase. This second minor endothermic peak appears at 140–150°C when the lithium salt is added. This minor endotherm is due to the melting of the crystalline complex phase formed between PEO and $LiCF_3SO_3$ [9,26,27]. The melting temperature (T_m) of crystalline PEO phase varies as shown in Fig. 5. The (T_m) of the $(PEO)_8LiCF_3SO_3$ system shifts initially towards higher temperature with increasing clay content and reaches a highest value at 9% clay, but decreases as the clay content is further increased.

Furthermore, the PEO crystallinity (X_c%) in the $(PEO)_8LiCF_3SO_3$/clay system is also altered with the addition of clay. The PEO crystallinity initially increases with increasing clay content, reaches a maximum value at 9% clay, and decreases as the clay content is further increased. However, the change of the glass transition temperature in this $(PEO)_8LiCF_3CF_3$/clay system cannot be observed in DSC analyses.

In order to clarify the phenomenon of increasing PEO crystallinity with the presence of small amount of clay, Fig. 6 shows plots of X_c% against clay content (wt%) with different EO/Li^+ ratios. X_c% has been calculated as a ratio of the heat enthalpy of the crystalline PEO phase to the heat enthalpy of the pure crystalline PEO (165.5 J g^{-1}) [9,26,27]. As can be seen, the X_c% of the undoped PEO system decreases gradually with increasing clay content, and this phenomenon can be attributed to a steric hindrance caused by huge surface area of the clay. A significant difference is observed when the lithium salt is added. In the samples with EO/Li^+ ratios of 8, 10 and 12, the PEO crystallinity increases initially with the increase in the clay content and approach maximum crystallinities at 9, 7 and 5% clay concentrations, respectively. Subsequently, the crystallinity decreases gradually with further increase in clay content. This observed trend in PEO crystallinity can be interpreted

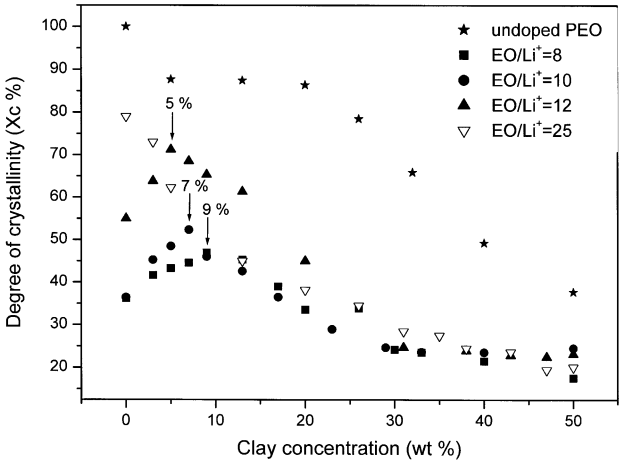

Fig. 6. Degree of crystallinity (X_c%) versus clay concentration (wt%) for PEO/clay/$LiCF_3SO_3$ composite electrolytes containing various EO/Li^+: (★) undoped PEO; (■) EO/Li^+ = 8; (●) EO/Li^+ = 10; (▲) EO/Li^+ = 12; (▽) EO/Li^+ = 25.

as the Lewis acid–base type interactions among polyether matrix, clay filler, lithium cation and corresponding anion. Three types of complexes can be assigned, which are depicted in Fig. 6. Complex I is present in the pure PEO phase and complex III is located within the clay phase. Complex II located at the interphase plays the key role in stabilizing these two microstructure phases. For the sample, EO/Li^+ = 8, 10 or 12, X_c% increases initially up to a specific clay concentration and then decreases. Without containing clay, the PEO/$LiCF_3SO_3$ system forms only the complex I. Portion of the complex I tends to convert into complex II and complex III, due to strong interaction existing between Li^+ cations and silicate layers of the clay. Shifting from complex I into complex II and complex III, portion of the original lithium cations have been drawn into the clay region and induces higher PEO chain flexibility and also higher crystallinity. In this aspect, the presence of clay causes higher PEO crystallinity due to greater PEO chain flexibility. However, more clay content results in forming more complex II and complex III, which can act as crystallization retarders (especially complex II) due to the steric hindrance and leads to lower PEO crystallinity. In this system, two adverse and competitive effects occur, one is favorable and other unfavorable for PEO crystallinity. As would be expected, higher Li^+ content (lower EO/Li^+ ratio) requires higher clay content, in order to reach the highest PEO crystallinity as demonstrated in Fig. 6. However, there is no critical clay concentration existed for the more diluted lithium salts system (EO/Li^+ = 25), the X_c% decreases progressively with the increase in the clay concentration as shown in Fig. 6. Similar trend is found in the undoped PEO system. Since the crystallinity of the diluted lithium salt system (EO/Li^+ = 25) is already very high (X_c = 80%), the unfavorable effect (steric hindrance) by adding clay, dominates the favorable effect (draw Li^+ into the clay region, Fig. 7) even with small quantity of the clay.

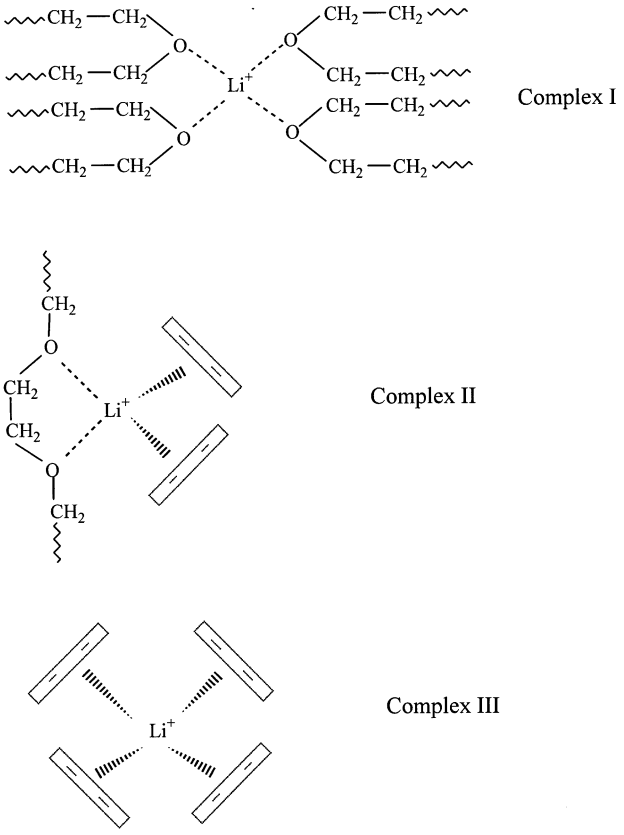

Fig. 7. Schematic structure of the complex formed by Li^+ cation with (a) polyether chains (complex I), (b) polyether and silicate layers (complex II), (c) silicate layers (complex III).

Therefore, the PEO crystallinity decreases progressively with the increase in the clay content, in this diluted lithium salt system.

3.4. FT-IR spectroscopy

FT-IR spectroscopy is a powerful tool for probing microscopic details in electrolytic systems, in particular, the characteristic $\nu_s(SO_3)$ internal mode of the $CF_3SO_3^-$ anion is sensitive in changing the local anionic environment [28–30]. According to prior literature [28–32], the component observed at ~1032 cm^{-1} has been assigned to the 'free' anion which does not interact directly with lithium cation. Components at ~1042 and ~1050–1054 cm^{-1} have been attributed to contact ion pairs and $Li_2CF_3SO_3^+$ triple ions (or ionic aggregates), respectively. Fig. 8 presents typical infrared spectra in the $\nu_s(SO_3)$ spectral region from 1015 to 1065 cm^{-1} at various EO/Li^+ ratios at 120°C, for the plain PEO and 3% clay electrolyte systems. The main peak shown in Fig. 8 tends to shift towards lower frequency, when 3% clay is added. This observed chemical shift could be attributed to the fact that the electron surrounding the lithium anion has been deprived by the addition of the clay. In other words, the attractive force between the lithium

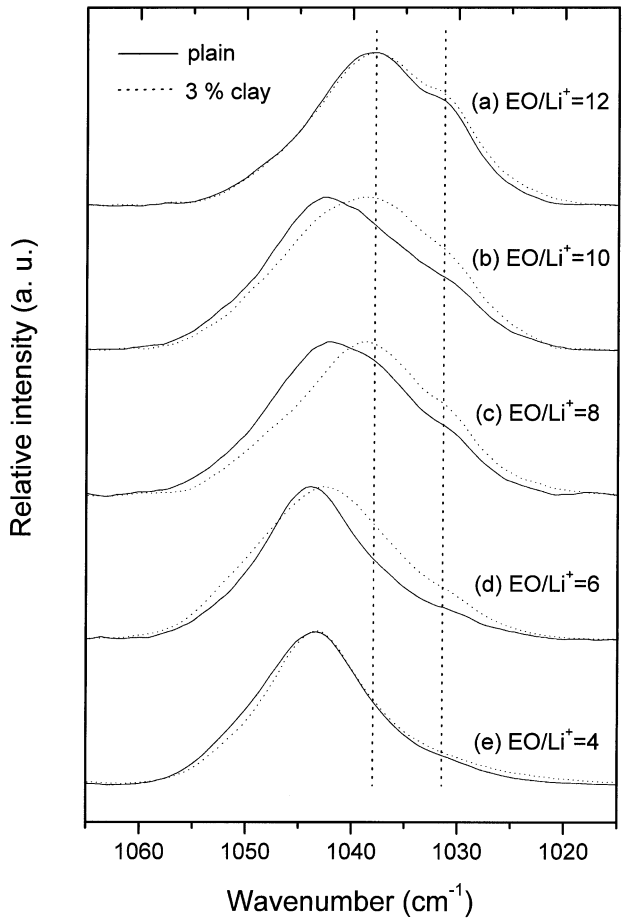

Fig. 8. Infrared spectra of $\nu_s(SO_3)$ internal modes for PEO/clay/$LiCF_3SO_3$ composite electrolytes: (—: plain system and: ····· 3 wt% clay) (a) $EO/Li^+ = 12$; (b) $EO/Li^+ = 10$; (c) $EO/Li^+ = 8$; (d) $EO/Li^+ = 6$; (e) $EO/Li^+ = 4$.

cation and anion is reduced by the negative charge in silicate layers.

Fractions of the 'free' anions, 'ionic pairs' and 'ionic aggregates' of the plain electrolyte and 3% clay electrolyte are measured by decompositing the $\nu_s(SO_3)$ band into three Gaussian peaks respectively. The results from curve fitting of Fig. 8 are summarized in Table 2, where the fraction of 'free' anions increases with the increase in the EO/Li^+ ratio in the both systems (plain electrolyte and 3% clay electrolyte).

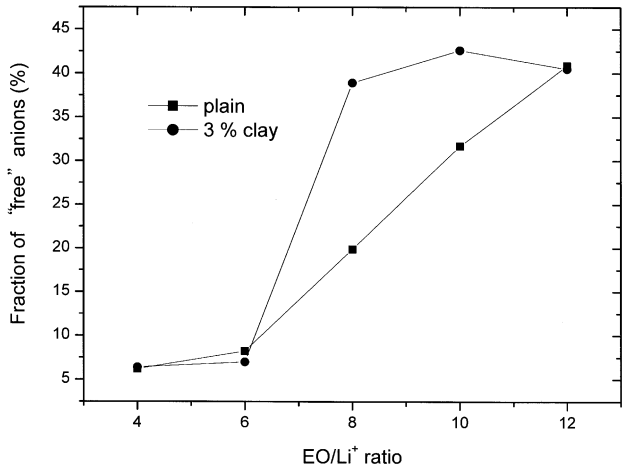

Fig. 9. Fraction of free anions versus EO/Li^+ ratio for PEO/clay/$LiCF_3SO_3$ composite electrolytes at 120°C: (■) PEO (100%)/clay (0%)/$LiCF_3SO_3$; (●) PEO (97%)/clay (3%)/$LiCF_3SO_3$; (concentration of PEO and clay in wt%).

In Fig. 9, the fraction of free anions is plotted against EO/Li^+ ratio. It is clearly seen that the fraction of free anions has a strong EO/Li^+ ratio dependence in the PEO/$LiCF_3CF_3$ plain system, a near linear relationship is evident. However, in the 3% clay electrolyte system, the fraction of free anions increases rapidly when the EO/Li^+ ratio is increased from 6 to 8 and approaches a plateau about 8. Variations of the free anion fraction can be attributed to the negative charges in the silicate layers that act the same function as the polar group in PEO to dissolve the lithium salt. In conclusion, the electrolyte containing 3% clay is most efficient in dissolving the lithium salt to produce highest fraction of free anions, than the plain electrolyte system. Notably, the fraction of free anions at high concentration of lithium salt ($EO/Li^+ = 4$ and 6) does not vary significantly in both systems, because of the insufficient negative charge supplied by the 3% clay.

4. Conclusions

This study has demonstrated that the addition of optimum content of D-2000 modified montmorillonite increases ionic

Table 2
Curve-fitting data of infrared spectra of symmetric SO_3 stretching mode, $\nu_s(SO_3)$, for PEO-based electrolyte composites with various EO/Li^+ mole ratio

symmetric SO_3 stretching mode, $\nu_s(SO_3)$						
EO/Li^+ ratio	PEO/LiTf			PEO(100)/clay(3)/LiTf		
	Free(%)	Pairs(%)	Aggr.(%)	Free(%)	Pairs(%)	Aggr.(%)
4	6.2	65.2	28.6	6.4	72.4	21.2
6	8.2	71.2	20.6	7	73.3	19.7
8	19.9	65.3	14.8	38.9	43.8	17.3
10	31.7	62.2	6.1	42.6	51.3	6.1
12	40.9	56.4	2.7	40.5	55.5	4

conductivity of the PEO based electrolyte by nearly sixteen times in comparison to the plain $(PEO)_8LiCF_3SO_3$ system. X-ray experiments have shown that the polymer nanocomposite was produced by the intercalation of the PEO chains within the silicate gallery. A.C. impedance, DSC and FT-IR studies indicated that strong interactions occur between the silicate layer and the dopant salt $LiCF_3SO_3$, within the PEO/clay/$LiCF_3SO_3$ system. These negative charges on the silicate layers interact with lithium cations to form two new types of complexes, which play the same role as the polar group in PEO. The presence of the clay tends to form complex II and III at the cost of complex I of the plain electrolyte by drawing Li^+ cations away from the PEO matrix. Reduced complex I will increase the chain flexibility of the polyether and it's crystallinity. However, an excess of clay tends to form more complex II and III and clutches the lithium cations tightly, and thus restricts the mobility of the cation and decreases the ionic conductivity. FT-IR spectra indicate that the existence of clay enhances the dissolution of the lithium salt and thus increases the fraction of free anion. However, the balanced attractive forces among silicate layers, ether groups and lithium cations produce an optimum ionic conductivity.

Acknowledgements

The authors would like to thank the Chinese Petroleum Corporation of the Republic of China for financially supporting this research under Contract No. NSC 89-CPC-7-009-007.

References

[1] Scrosati B. In: MacCallum JR, Vincent CA, editors. Polymer electrolyte reviews. New York: Elsevier, 1989. p. 315.
[2] Scrosati B. In: Scrosati B, editor. Applications of electroactive polymers. New York: Chapman and Hall, 1993. p. 251.
[3] Armand MB. Solid State Ionics 1983;9–10:745.
[4] Chao S, Wrighton MS. J Am Chem Soc 1987;109:2197.
[5] Fenton DE, Parker JM, Wright PV. Polymer 1973;7:319.
[6] Ratner MA, Shriver DF. Chem Rev 1988;88:109.
[7] Wang Li, Yang B, Wang XL, Tang XZ. J Appl Polym Sci 1999;71:1711.
[8] Wang XL, Li H, Tang XZ, Chang FC. J Polym Sci B, Polym Phys 1999;37:837.
[9] Wieczorek W, Raducha D, Zalewska A, Stevens JR. J Phys Chem B 1998;102:8725.
[10] Abraham KM, Jiang Z, Carroll B. Chem Mater 1997;9:1978.
[11] Yang XQ, Hanson L, McBreen J, Okamoto Y. J Power Sources 1995;54:198.
[12] Lee JC, Litt MH. Macromolecules 2000;33:1618.
[13] Labreche C, Levesque I, Prud'homme J. Macromolecules 1996;29:7795.
[14] Mishra R, Rao KJ. Solid State Ionics 1998;106:113.
[15] Scanlon LG, Giannelis EP. Adv Mater 1995;7:154.
[16] Ogata N, Kawakage S, Ogihara T. Polymer 1997;38:5115.
[17] Kumar B, Scanlon LG. Solid State Ionics 1999;124:239.
[18] Croce F, Appetecchi GB, Persi L, Scrosati B. Nature 1998;394:456.
[19] Kloster GM, Thomas JA, Brazis PW, Kannewurf CR, Shriver DF. Chem Mater 1996;8:2418.
[20] Wieczorek W, Florjanczyk Z, Stevens JR. Electrochim Acta 1995;40:2251.
[21] Wieczorek W, Such K, Chung SH, Stevens JR. J Phys Chem 1994;98:9047.
[22] Ogata N, Kawakage S, Ogihara T. Polymer 1997;38:5115.
[23] Vaia RA, Vasudevan S, Krawiec W, Scanlon LG, Giannelis EP. Adv Mater 1995;7:154.
[24] Jeevanandam P, Vasudevan S. Chem Mater 1998;10:1276.
[25] Wong S, Zax DB. Electrochim Acta 1997;42:3513.
[26] Wieczorek W, Zalewska A, Raducha D, Florjanczyk Z, Stevens JR. Macromolecules 1996;29:143.
[27] Wieczorek W, Zalewska A, Raducha D, Florjanczyk Z, Stevens JR. J Phys Chem B 1998;10:352.
[28] Huang W, Frech R, Wheeler RA. J Phys Chem 1994;98:100.
[29] Ferry A, Edman L, Forsyth M, MacFarlane DR, Sun J. J Appl Phys 1999;86:2346.
[30] Ferry A. J Phys Chem B 1997;101:150.
[31] Huang W, Frech R. Polymer 1994;35:235.
[32] Jin JH, Hong SU, Won J, Kang YS. Macromolecules 2000;33:4932.